ISSN 0965-5425, Computational Mathematics and Mathematical Physics, 2023, Vol. 63, No. 7, pp. 1341–1349. © Pleiades Publishing, Ltd., 2023.
Russian Text © The Author(s), 2023, published in Zhurnal Vychislitel'noi Matematiki i Matematicheskoi Fiziki, 2023, Vol. 63, No. 7, pp. 1216–1224.

MATHEMATICAL PHYSICS

# On the Accuracy of Shock-Capturing Schemes Calculating Gas-Dynamic Shock Waves

**V. A. Kolotilov[a],*, A. A. Kurganov[b,c],**, V. V. Ostapenko[a],***, N. A. Khandeeva[a],****, and S. Chu[b],*******

[a] *Lavrentyev Institute of Hydrodynamics, Siberian Branch, Russian Academy of Sciences, Novosibirsk, 630090 Russia*

[b] *Department of Mathematics, Southern University of Science and Technology, Shenzhen, 518005 China*

[c] *Shenzhen International Center for Mathematics and Guangdong Provincial Key Laboratory of Computational Science and Material Design, Southern University of Science and Technology, Shenzhen, 518005 China*

**e-mail: kolotilov1992@gmail.com*

***e-mail: alexander@sustech.edu.cn*

****e-mail: ostapenko_vv@ngs.ru*

*****e-mail: nzyuzina1992@gmail.com*

******e-mail: chuss2019@mail.sustech.edu.cn*

Received December 9, 2022; revised December 9, 2022; accepted March 30, 2023

**Abstract**—A comparative experimental accuracy study of three shock-capturing schemes (the second-order CABARET, third-order Rusanov, and fifth-order in space third-order in time A-WENO schemes) is carried out by numerically solving a Cauchy problem with smooth periodic initial data for the Euler equations of gas dynamics. In the studied example, the solution breaks down and shock waves emerge. It is shown that the CABARET and A-WENO schemes, which are constructed using nonlinear limiters as a stabilization mechanism, have approximately the same accuracy in the areas of shock wave influence, while the nonmonotone Rusanov scheme has significantly higher accuracy in these areas despite producing noticeable nonphysical oscillations in the immediate vicinities of shock waves. At the same time, the combined scheme obtained based on the Rusanov and CABARET schemes localizes shock wave fronts, which are captured in a non-oscillatory manner, and preserves higher accuracy in the areas of the shock influence.

**Keywords:** gas dynamic equations, shock waves, high-order shock-capturing schemes

**DOI:** 10.1134/S0965542523070060

## 1. INTRODUCTION

Since it was shown in the classic work [1] that there were no high-order two-level monotone schemes, the development of numerical methods for hyperbolic systems of conservation laws was focused on overcoming this "Godunov barrier". As a result, many classes of numerical methods proposed in [2–9] achieve both high order of accuracy on smooth solutions and monotonicity with the help of nonlinear flux correction (NFC). Main classes of the NFC schemes include MUSCL [10], TVD [11], Central [12], WENO [13], DG (Discontinuous Galerkin) [2, 3], and CABARET [14] schemes.

In [16], an example of shallow water equations [15] was studied and it was shown that in the shock influence regions, NFC schemes achieved at most first order of both local and integral (on intervals with at least one of the endpoint lying inside a shock influence region) convergence [17–19]. At the same time, some high-order nonmonotone schemes (in particular, the Rusanov scheme [20] and the compact scheme from [16]) maintain a high order of integral convergence in the negative norm when the integration is performed over the domains containing strong discontinuities [17, 18]. As a result, these nonmonotone schemes, achieve substantially higher (compared with the NFC schemes) accuracy in shock influence regions despite noticable oscillations at shock fronts.

In [17–19], a method of constructing combined schemes was developed and applied to the shallow water equations. These schemes combine the advantages of both NFC and classical nonmonotone schemes: They localize shock waves and capture their frons in a non-oscillatory manner and at the same time maintain a high order of accuracy in the shock influence regions. In combined schemes, a high-order

nonmonotone scheme ("basic scheme") is first used to compute the solution in the entire computational domain. Then, in the neighborhoods of large solution gradients, where the basic scheme produces nonphysical oscillations, the oscillatory solution is corrected by numerically solving the corresponding initial-boundary value problems using one of the NFC schemes as an "internal scheme".

The combined schemes in [17] use the third-order weak approximation implicit scheme [16] as a basic scheme, while in [18], the third-order explicit Rusanov scheme [20] was utilized as a basic scheme. In both [17, 18], a monotonized version of the second-order CABARET scheme [4] is used as an internal scheme. The combined scheme in [19] uses a nonmonotone third-order DG method as a basic scheme and a monotonized, NFC-based version of the same DG method [2] as an internal scheme.

In this paper, we study the accuracy of several schemes for the Euler equations of gas dynamics [21], which, unlike the shallow water equations, are not genuinely nonlinear [22] (since it has a linearly degenerate characteristic field and thus admits contact discontinuities) and, in general, cannot be rewritten in terms of the Riemann invariants. We perform a comparative accuracy study of the Rusanov [19] and two different modern NFC schemes (a monotonized modification of the CABARET scheme [23] and the A-WENO scheme from [24]) on a numerical example, in which shock waves emerge out of the smooth periodic initial data. In this example, the solution breaks down and a sequence of isolated shock waves propagating with a constant speed is formed. As a result, shock influence regions appear between the shock waves and as time progresses, these regions expand and eventually cover the entire computational domain.

Our numerical experiments demonstrate that the local accuracy of all of the studied schemes at smooth parts of the computed solution located away from the shock influence regions corresponds to their formal order of accuracy: The Rusanov scheme is more accurate than the CABARET scheme, and the A-WENO scheme is much more accurate than the Rusanov scheme. At the same time, inside shock influence regions, the local accuracy of the both NFC schemes (CABARET and A-WENO) is about the same and it is substantially lower than the local accuracy of the nonmonotone Rusanov scheme, which, in turn, develops noticable nonphysical oscillations in the vicinity of the shock fronts. We give a theoretical justification of the obtained numerical results.

Similarly to [18], we construct a combined scheme for the Euler equations of gas dynamics. In our scheme, the Rusanov scheme is used as a basic scheme and the CABARET scheme serves as an internal scheme, which is applied in the areas of large gradients detected with the help of the method proposed in [25]. The resulting combined scheme localizes shock wave fronts in a monotone, non-oscillatory manner and, at the same time, maintains high order of accuracy in the shock influence areas.

## 2. METHODS OF ACCURACY ESTIMATION

Consider quasilinear hyperbolic systems of conservation laws, which read as [21, 22]:

$$\mathbf{u}_t + \mathbf{f}(\mathbf{u})_x = \mathbf{0}, \tag{2.1}$$

where $\mathbf{u}(x,t)$ is a vector of unknowns and $\mathbf{f}(\mathbf{u})$ is a smooth $m$-dimensional flux vector function. We assume that the system (2.1) is strictly hyperbolic, which means that all of the eigenvalues $\lambda_i(\mathbf{u})$ of the Jacobian $A(\mathbf{u}) = \mathbf{f}_\mathbf{u}(\mathbf{u})$ are real and distinct. We consider the system (2.1) subject to the periodic initial data

$$\mathbf{u}(x,0) = \mathbf{u}_0(x) = \mathbf{u}_0(x+X), \tag{2.2}$$

where $\mathbf{u}_0(x)$ is a given vector function, and $X$ is the period. We assume that the initial value problem (2.1), (2.2) has a unique weak solution $\mathbf{u}(x,t)$, which is bounded, but breaks down at a certain time $t > 0$ and develops shock waves.

We will construct explicit numerical methods for the initial value problem (2.1), (2.2) on the unifrom Cartesian grid

$$S = \{(x_j, t_n) : x_j = jh,\ t_n = n\tau,\ n \geq 0\}, \tag{2.3}$$

where $h = X/M$ is a spatial stepsize, $M$ is a given positive number,

$$\tau = zh/\max_{k,j,n}\left|\lambda_k(\mathbf{v}_h(x_{j+1/2}, t_n))\right|, \tag{2.4}$$

is a timestep selected using the CFL condition with the CFL number $z \in (0,1)$, and $\mathbf{v}_h(x_{j+1/2}, t_n)$ is a computed solution at the node $x_{j+1/2} = (j+1/2)h$ with the semi-integer spatial superscript. In applied computations, one can naturally save the CPU time by using nonuniform temporal grids

$$\bar{S} = \{(x_j, t_n) : x_j = jh,\ t_{n+1} = t_n + \tau_n,\ t_0 = 0\},$$

in which the timestep $\tau_n$ is determined according to

$$\tau_n = zh/\max_{k,j}\left|\lambda_k(\mathbf{v}_h(x_{j+1/2}, t_n))\right|.$$

However, since the main goal of this work is to study the experimental convergence rates of several numerical methods, it is more convenient to use the uniform grid (2.3) with the constant timestep (2.4).

As in the numerical example, which will be considered below, no exact solution $\mathbf{u}(x,t)$ of the studied Cauchy problem (2.1), (2.2) is available, we will compute the error in the computation of the numerical solution $\mathbf{v}_h(x_{j+1/2}, t_n)$ on the basic grid (2.3) with the help of the reference solution, which will be obtained by taking an odd number $N \gg M$ and computing a quasi-exact solution $\mathbf{v}_{h_*}(x^*_{j+1/2}, t^*_n)$ by one of the high-order schemes on a substantially finer uniform grid

$$S_* = \{(x^*_j, t^*_n) : x^*_j = jh_*,\ t^*_n = n\tau^*,\quad n \geq 0\}, \tag{2.5}$$

where $x^*_{j+1/2} = (j+1/2)h_*$, $h_* = h/N$, and $\tau_* = \tau/N$. As a result, the error in the numerical solution $\mathbf{v}_h$ at the node $(x_{j+1/2}, t_n)$ of the basic grid (2.3) will be approximated by

$$\delta\mathbf{v}_h(x_{j+1/2}, t_n) = \mathbf{v}_h(x_{j+1/2}, t_n) - \mathbf{v}_{h_*}(x^*_{(j+1/2)N}, t^*_{nN}). \tag{2.6}$$

In the figures below, we will show the relative disbalances (errors) in the computation of the vector solution $\mathbf{u}$, determined by

$$\Delta\mathbf{v}_h(x_{j+1/2}, t_n) = \log\frac{|\delta\mathbf{v}_h(x_{j+1/2}, t_n)|}{|\mathbf{v}_{h_*}(x^*_{(j+1/2)N}, t^*_{nN})|}. \tag{2.7}$$

If the hyperbolic system (2.1) models a certain physical process, formula (2.7) will be correct only if the system (2.1) is dimensionless. If the dimensional units are used, then formula (2.7) will be correct provided the components of the vectors $\mathbf{v}_h$ and $\mathbf{v}_{h_*}$ in formulae (2.6) and (2.7) are replaced with their dimensionless analogs.

## 3. TEST PROBLEM

We consider the dimensionless Euler equations of gas dynamics [4, 21], which read as the hyperbolic system (2.1) with

$$\mathbf{u} = \begin{pmatrix} \rho \\ \rho u \\ \rho e \end{pmatrix}, \quad \mathbf{f}(\mathbf{u}) = \begin{pmatrix} \rho u \\ \rho u^2 + p \\ u(\rho e + p) \end{pmatrix}, \tag{3.1}$$

where $\rho$, $u$, $p$, and $e = \varepsilon + u^2/2$ are the density, velocity, pressure, and specific total energy, respectively, and $\varepsilon$ is the specific internal energy. The pressure and internal energy satisfy the equation of state for an ideal polytropic gas

$$p = (\gamma - 1)\rho\varepsilon, \tag{3.2}$$

in which $\gamma = 1.4$ is the specific heat ratio of diatomic gas. When $\rho > 0$ and $p > 0$, the system (2.1), (3.1), (3.2), is strictly hyperbolic since its Jacobian has three real and distinct eigenvalues

$$\lambda_1 = u - c, \quad \lambda_2 = u, \quad \lambda_3 = u + c,$$

where $c = \sqrt{\gamma p/\rho}$ is the adiabatic speed of sound.

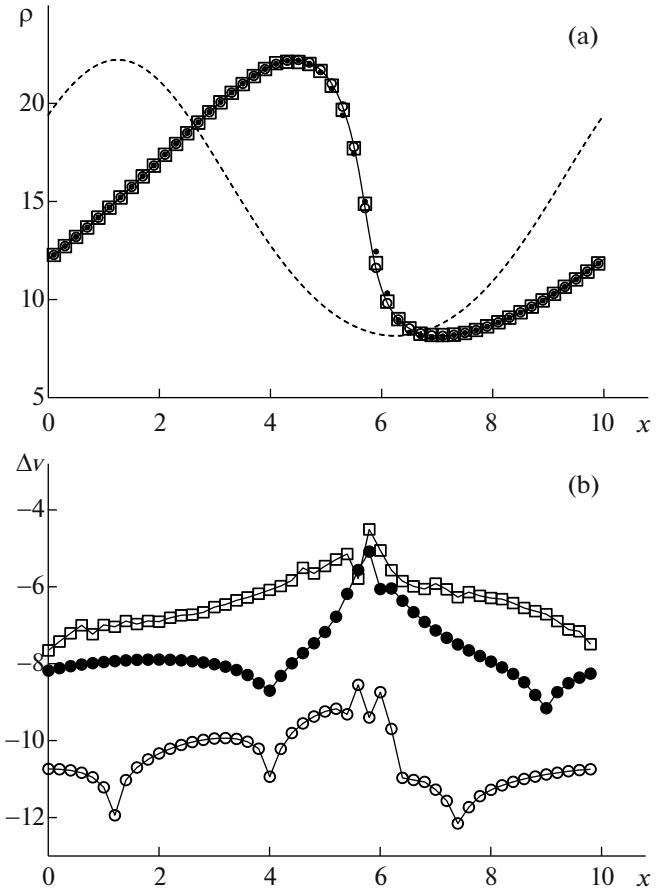


**Fig. 1.** Gas density (a) and relative local disbalances (b) obtained at the time moment $t = 1$ in the numerical solution of the Cauchy problem (2.1), (3.1), (3.3), (3.4) using the CABARET (squares), Rusanov (dots) and A-WENO (mugs) schemes. In the graph (a), the solid line shows the quasi-exact, and the dotted line shows the initial density values.

We consider the system (2.1), (3.1) subject to the smooth periodic initial data

$$u(x,0) = \sin\left(\frac{2\pi x}{X} + \frac{\pi}{4}\right), \tag{3.3}$$

$$\rho(x,0) = \left(\frac{\gamma-1}{2\sqrt{\gamma}}\big(u(x,0)+10\big)\right)^{2/(\gamma-1)}, \quad p(x,0) = \big(\rho(x,0)\big)^{\gamma}, \tag{3.4}$$

where $X = 10$ is the period. Formulae (3.3) and (3.4) imply that the entropy

$$s = \frac{1}{\gamma-1}\ln\frac{p}{\rho^{\gamma}},$$

which is the invariant $w_2$ of the system (2.1), (3.1), and the isentropic quasi-invariants [7] of this system

$$w_1 = u - \frac{2c}{\gamma-1}, \quad w_3 = u + \frac{2c}{\gamma-1},$$

have the following initial values:

$$w_1(x,0) = -10, \quad s(x,0) = 0, \quad w_3(x,0) = 2\sin\left(\frac{2\pi x}{X} + \frac{\pi}{4}\right) + 10. \tag{3.5}$$

Since initially the entropy is constant, the flow in the smooth parts of the exact solution (those are not in the shock influence areas) is isentropic. We note that due to (3.5), the initial value problem (2.1), (3.1), (3.3), (3.4) is analogous to the Cauchy problem for the shallow water equations studied in [17–19].

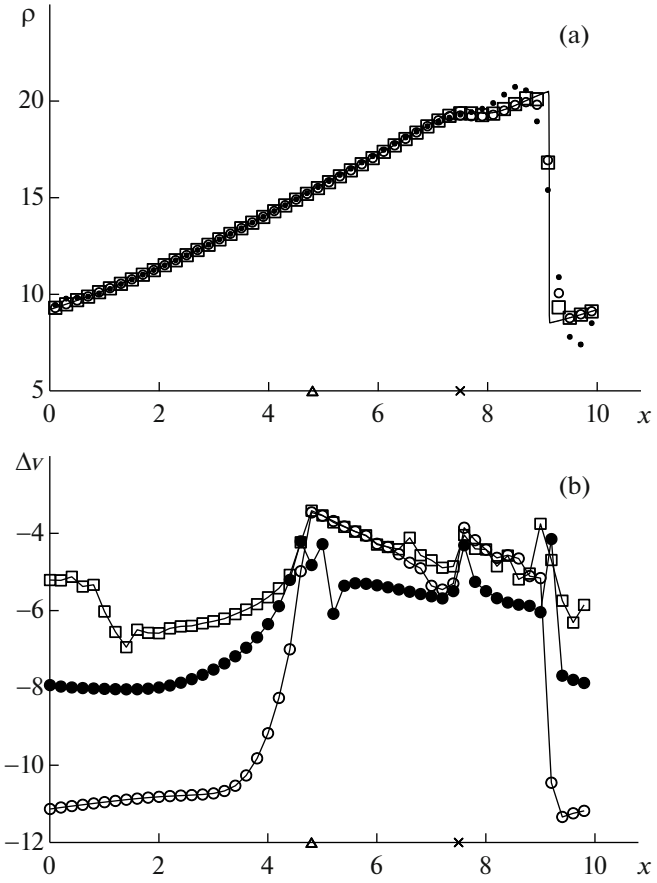


**Fig. 2.** Gas density (a) and relative local disbalances (b) obtained at the time moment $t = 2.5$ in the numerical solution of the Cauchy problem (2.1), (3.1), (3.3), (3.4) using the CABARET (squares), Rusanov (dots) and A-WENO (mugs) schemes. The cross marks the coordinate of the weak contact discontinuity, and the triangle depicts the left boundary of the domain of influence of the shock wave. In the graph (a), the solid line shows the quasi-exact, and the dotted line shows the initial density values.

At the time moment $t_* \approx 1.35$, the exact solution of the initial value problem (2.1), (3.1), (3.3), (3.4) develops a sequence of isolated shock waves, which propagate one after the other with the same speeds in the positive direction of the $x$-axis so that the distance between the consecutive shock waves remains constant in time and is equal to the period $X$. In Fig. 1a, the initial density given by (3.5), is plotted by the dashed line, and in Figs. 1a, 2a, 3a, and 4a, the reference densities, computed by the A-WENO scheme [24] on a very fine grid (2.5) with $h_* = 0.005$ and $\tau_* = 0.0005$ at the times $t = 1$, $t = 2.5$, $t = 3.5$, and $t = 5$, are plotted by the continuous lines. By the time $t = 1$, the exact solution starts developing large gradients, but the solution still remains smooth (Fig. 1a). The shock waves, which merge at the time moment $t_*$ as strong discontinuities of initially infinitely small magnitude, have finite magnitude (Fig. 2a) at the time $t = 2.5$, but their domains of influence, located inside the intervals $(10i + 5, 10i + 9) \subset [10i, 10i + 10]$, $i \in \mathbb{Z}$, still do not fill the entire computational domain. By the time moment $t = 3.5$, the shock waves travel the distance larger than the period $X = 10$ and the entire computational domain becomes the shock influence area. Thus, the strong discontinuities that can be seen in Figs. 3a and 4a, correspond to the shock wave that had formed at the time moment $t_*$ within the interval $[-X, 0]$.

## 4. NUMERICAL RESULTS

In Figs. 1–4, we show the numerical solutions of the Cauchy problem (2.1), (3.1), (3.3), (3.4) computed using the CABARET (squares), Rusanov (dots), and A-WENO (circles) schemes on the uniform

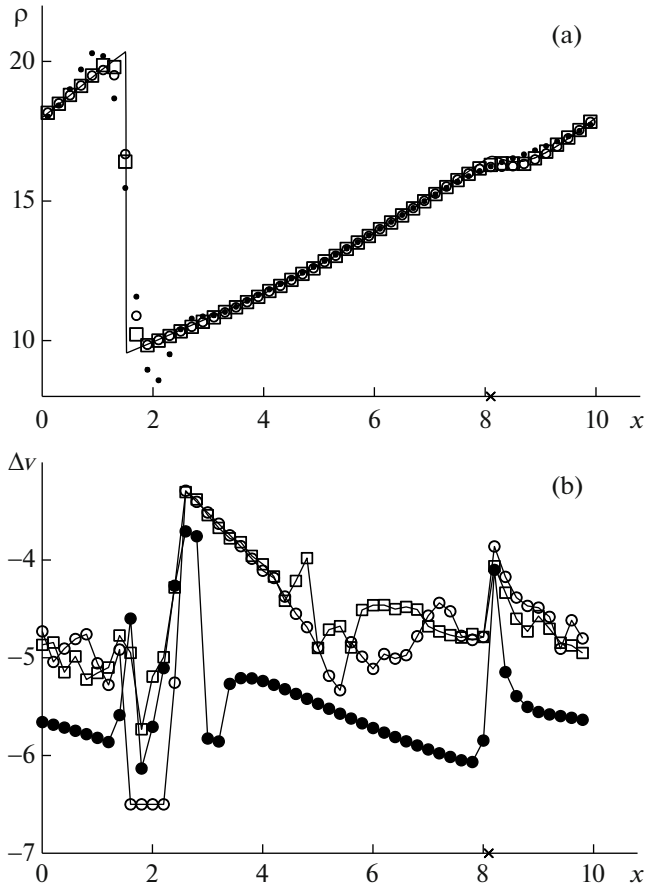


**Fig. 3.** Gas density (a) and relative local disbalances (b) obtained at the time moment $t = 3.5$ in the numerical solution of the Cauchy problem (2.1), (3.1), (3.3), (3.4) using the CABARET (squares), Rusanov (dots) and A-WENO (mugs) schemes. The cross marks the coordinate of the weak contact discontinuity. In the graph (a), the solid line shows the quasi-exact, and the dotted line shows the initial density values.

grid (2.3) with the timestep selected by the stability condition (2.4) with the CFL number $z \approx 0.35$. In the top panels marked by the index (a), the densities computed on the grid (2.3) with the spatial stepsize $h = 0.2$, are shown. One can see that unlike the NFC (CABARET and A-WENO) schemes, the Rusanov scheme develops noticable nonphysical oscillations in the neighborhoods of the shock waves.

In the bottom panels marked by the index (b), we plot the relative local disbalances (2.7), obtained on the basic grid (2.3) with the spatial stepsize $h = 0.005$. In formula (2.7), the reference solution was computed using the Rusanov scheme [20] on the fine grid (2.5) with $h_* = 2.4\times10^{-4}$ and $\tau_* = 2.4\times10^{-5}$. These results are shown for each 40th spatial node $j = 40i$ of the basic grid (2.3). As can be seen in Figs. 1b and 2b, outside the shock influence regions the A-WENO scheme is about two-three orders of magnitude more accurate than the Rusanov scheme and about three-four orders of magnitude more accurate than the CABARET scheme. Inside the shock influence domains, the accuracy of the A-WENO scheme sharply deteriorates (Figs. 2b, 3b, and 4b), becomes comparable with the accuracy of the CABARET scheme and substantially lower than the accuracy of the Rusanov scheme. As time progresses, the difference in the accuracy between the Rusanov and A-WENO schemes noticably increases riching by the time moment $t = 5$ (Fig. 4b) about one and a half orders of magnitude in the main part of the smooth solution region. It should be observed that the accuracy of all of the studied schemes sharply deteriorates not only in the vicinity of the shock front, but also near the weak contact discontinuity, whose location is marked by the crosses on the $x$-axis.

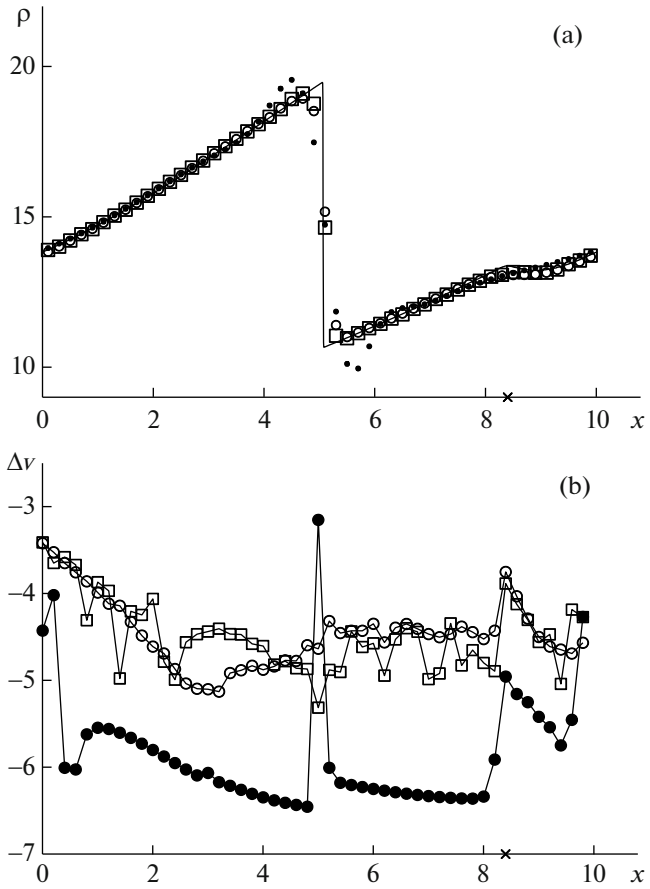


**Fig. 4.** Gas density (a) and relative local disbalances (b) obtained at the time moment $t = 5$ in the numerical solution of the Cauchy problem (2.1), (3.1), (3.3), (3.4) using the CABARET (squares), Rusanov (dots) and A -WENO (mugs) schemes. The cross marks the coordinate of the weak contact discontinuity. In the graph (a), the solid line shows the quasi-exact, and the dotted line shows the initial density values.

## 5. A COMBINED SCHEME

Using the methodology proposed in [17], and similarly to [18], we construct a combined CRC (Combined Rusanov–CABARET) scheme for the Euler equations of gas dynamics (2.1), (3.1). In the CRC scheme, the Rusanov scheme is a basic scheme and the CABARET scheme is the internal scheme. The large gradient regions, in which the internal scheme is applied, are detected with the help of the method proposed in [25]. The densities obtained by the CRC scheme on the grid (2.3) with the spatial stepsize $h = 0.2$ are visually close to those obtained using the CABARET scheme, while the relative local disbalances (2.7) obtained by the CRC scheme on the basic grid (2.3) with the spatial stepsize $h = 0.005$ are visually close to those obtained using the Rusanov scheme. Therefore, the CRC scheme localizes the shock fronts in a monotone, non-oscillatory way and, at the same time, maintains high order of accuracy in the shock influence regions.

## 6. DISCUSSION OF THE OBTAINED RESULTS

The results shown in Figs. 1–4 demonstrate that as in the numerical simulations of discontinuous solutions of the shallow water equations [17–19], the accuracy of the NFC schemes of different formal orders becomes about the same in the shock influence regions. Moreover, their accuracy is substantially lower than the accuracy of the Rusanov scheme. This drawback of the NFC schemes is directly related to their main advantage—monotone localization of shock fronts, since a partial sum of the Fourier expansion of a discontinuous function is not a monotone function. Therefore, the oscillations developed at the shock fronts in the numerical solutions obtained by the nonmonotone Rusanov scheme, carry the information about the Fourier wave structure in the vicinities of strong discontinuities: This allows the Rusanov

scheme to accurately approximate the Rankine–Hugoniot conditions and, as a result, to maintain high accuracy in the shock influence regions. On the contrary, the NFC schemes lose this information due to the artificial shock wave smearing, and this leads to the reduction in the accuracy in the approximation of the Rankine–Hugoniot conditions.

At the same time, numerical solutions of the initial value problem (2.1), (3.1), (3.3), (3.4) demonstrate that the Rusanov scheme (as well as the NFC CABARET and A-WENO schemes) exhibits only first order of integral convergence in the negative norm on the intervals with one of the endpoints lying in the shock influence region. This is a major difference from the numerical results reported in [18], where the Rusanov scheme (unlike the NFC schemes) maintained the second order of integral convergence and this ensured the accuracy of the Rusanov scheme to be about three orders of magnitude higher compared with the NFC schemes in the shock influence regions. As a result, when the Cauchy problem (2.1), (3.1), (3.3), (3.4) is numerically solved, the advantage of the Rusanov scheme in terms of its accuracy in the shock influence regions (compared with the CABARET and A-WENO schemes) reduces to about one and a half orders of magnitude. This advantage, however, is still quite essential and this allows us to recommend the combined CRC scheme (based on the Rusanov scheme) proposed in the previous section, to be used for numerical simulations of more complicated gas dynamics flows.

## FUNDING

The reported study was partially funded by the RSF project no. 22-11-00060 (Sections 1–3) and also by RFBR and NSFC project nos. 21-51-53012 (RFBR) and 12111530004 (NSFC) (Sections 4–6). The development of A-WENO scheme was supported by NSFC grant no. 12171226 and also by the fund of the Guangdong Provincial Key Laboratory of Computational Science and Material Design (no. 2019B030301001).

## CONFLICT OF INTEREST

The authors declare that they have no conflicts of interest.

## REFERENCES

1. S. K. Godunov, "Difference method for computing discontinuous solutions of fluid dynamics equations," Mat. Sb. **47** (3), 271–306 (1959).
2. B. Cockburn, "An introduction to the discontinuous Galerkin method for convection-dominated problems, advanced numerical approximation of nonlinear hyperbolic equations," Lect. Notes Math. **1697**, 150–268 (1998). https://doi.org/10.1007/BFb0096353
3. B. Cockburn and C.-W. Shu, "Runge–Kutta discontinuous Galerkin methods for convection-dominated problems," J. Sci. Comput. **16** (3), 173–261 (2001). https://doi.org/10.1023/A:1012873910884
4. A. G. Kulikovskii, N. V. Pogorelov, and A. Yu. Semenov, *Mathematical Aspects of Numerical Solution of Hyperbolic Systems* (Fizmatlit, Moscow, 2001; Chapman and Hall/CRC, London, 2001).
5. R. J. LeVeque, *Finite Volume Methods for Hyperbolic Problems* (Cambridge Univ. Press, Cambridge, 2002). https://doi.org/10.1017/CBO9780511791253
6. E. F. Toro, *Riemann Solvers and Numerical Methods for Fluid Dynamics: A Practical Introduction* (Springer, Berlin, 2009). https://doi.org/10.1007/b79761
7. V. M. Goloviznin, M. A. Zaitsev, S. F. Karabasov, and I. A. Korotkin, *New CFD Algorithms for Multiprocessor Computer Systems* (Mosk. Gos. Univ., Moscow, 2013) [in Russian].
8. J. S. Hesthaven, *Numerical Methods for Conservation Laws* (SIAM, Philadelphia, 2018). https://doi.org/10.1137/1.9781611975109
9. C.-W. Shu, "Essentially non-oscillatory and weighted essentially non-oscillatory schemes," Acta Numer. **29**, 701–762 (2020). https://doi.org/10.1017/S0962492920000057
10. B. Van Leer, "Toward the ultimate conservative difference scheme: V. A second-order sequel to Godunov's method," J. Comput. Phys. **32** (1), 101–136 (1979). https://doi.org/10.1016/0021-9991(79)90145-1
11. A. Harten, "High resolution schemes for hyperbolic conservation laws," J. Comput. Phys. **49**, 357–393 (1983). https://doi.org/10.1016/0021-9991(83)90136-5
12. H. Nessyahu and E. Tadmor, "Non-oscillatory central differencing for hyperbolic conservation laws," J. Comput. Phys. **87** (2), 408–463 (1990). https://doi.org/10.1016/0021-9991(90)90260-8

13. X.-D. Liu, T. Osher, and T. Chan, "Weighted essentially non-oscillatory schemes," J. Comput. Phys. **115** (1), 200–212 (1994).
https://doi.org/10.1006/jcph.1994.1187
14. S. A. Karabasov and V. M. Goloviznin, "Compact accurately boundary-adjusting high-resolution technique for fluid dynamics," J. Comput. Phys. **228**, 7426–7451 (2009).
https://doi.org/10.1016/j.jcp.2009.06.037
15. J. J. Stoker, *Water Waves* (Wiley, New York, 1957).
16. V. V. Ostapenko, "Construction of high-order accurate shock-capturing finite-difference schemes for unsteady shock waves," Comput. Math. Math. Phys. **40** (12), 1784–1800 (2000).
17. O. A. Kovyrkina and V. V. Ostapenko, "On the construction of combined finite-difference schemes of high accuracy," Dokl. Math. **97** (1), 77–81 (2018).
https://doi.org/10.1134/S1064562418010246
18. N. A. Zyuzina, O. A. Kovyrkina, and V. V. Ostapenko, "Monotone finite-difference scheme preserving high accuracy in regions of shock influence," Dokl. Math. **98** (2), 506–510 (2018).
https://doi.org/10.1134/S1064562418060315
19. M. E. Ladonkina, O. A. Neklyudova, V. V. Ostapenko, and V. F. Tishkin, "Combined DG scheme that maintains increased accuracy in shock wave areas," Dokl. Math. **100** (3), 519–523 (2019).
https://doi.org/10.1134/S106456241906005X
20. V. V. Rusanov, "Third-order accurate shock-capturing schemes for computing discontinuous solutions," Dokl. Akad. Nauk SSSR **180** (6), 1303–1305 (1968).
21. B. L. Rozhdestvenskii and N. N. Yanenko, *Systems of Quasilinear Equations and Their Applications to Gas Dynamics* (Nauka, Moscow, 1978; Am. Math. Soc., Providence, R.I., 1983).
22. P. D. Lax, *Hyperbolic Systems of Conservation Laws and the Mathematical Theory of Shock Waves* (SIAM, Philadelphia, 1972).
23. V. V. Ostapenko and V. A. Kolotilov, "Application of the CABARET scheme for calculating discontinuous solutions of a hyperbolic system of conservation laws," Dokl. Math. **104** (3), 369–373 (2021).
https://doi.org/10.1134/S1064562421060120
24. B.-S. Wang, W. S. Don, A. Kurganov, and Y. Liu, "Fifth-order A-WENO schemes based on the adaptive diffusion central-upwind Rankine–Hugoniot fluxes," Commun. Appl. Math. Comput. (2021).
https://doi.org/10.1007/s42967-021-00161-2
25. S. Karni, A. Kurganov, and G. Petrova, "A smoothness indicator for adaptive algorithms for hyperbolic systems," J. Comput. Phys. **178**, 323–341 (2002).
https://doi.org/10.1006/jcph.2002.7024